Radiofluorinated N-Octanoyl Dopamine ([F-18]F-NOD) as a Tool To Study Tissue Distribution and Elimination of NOD in Vitro and in Vivo

Pretze, Marc; Pallavi, Prama; Roscher, Mareike; Klotz, Sarah; Caballero, Julio; Binzen, Uta; Greffrath, Wolfgang; Treede, Rolf-Detlef; Harmsen, Martin C; Hafner, Mathias

Published in:
Journal of Medicinal Chemistry

DOI:
10.1021/acs.jmedchem.6b01191

Journal of Medicinal Chemistry

Article

pubs.acs.org/jmc

Radiofluorinated *N*-Octanoyl Dopamine ([^{18}F]F-NOD) as a Tool To Study Tissue Distribution and Elimination of NOD in Vitro and in Vivo

Marc Pretze,*[,†,○] Prama Pallavi,[‡,#,○] Mareike Roscher,[†] Sarah Klotz,[‡] Julio Caballero,[§] Uta Binzen,[∥] Wolfgang Greffrath,[∥] Rolf-Detlef Treede,[∥] Martin C. Harmsen,[⊥] Mathias Hafner,[#] Benito Yard,[‡] Carmen Wängler,[▽] and Björn Wängler*[,†]

[†]Molecular Imaging and Radiochemistry, Department of Clinical Radiology and Nuclear Medicine, [‡]V. Department of Medicine, Nephrology, University Hospital Mannheim, [∥]Division of Neurophysiology, Center of Biomedicine and Medical Technology Mannheim (CBTM), [▽]Biomedical Chemistry, Department of Clinical Radiology and Nuclear Medicine, Medical Faculty Mannheim of Heidelberg University, Theodor-Kutzer-Ufer 1-3, Mannheim 68167, Germany

[§]Center for Bioinformatics and Molecular Simulations, Faculty of Engineering in Bioinformatics, Universidad de Talca, Talca 07101, Chile

[⊥]University of Groningen, University Medical Center Groningen, Department of Pathology and Medical Biology, Groningen 9713 GZ, The Netherlands

[#]Institute for Molecular and Cellular Biology, Mannheim University of Applied Sciences, Mannheim 68163, Germany

Supporting Information

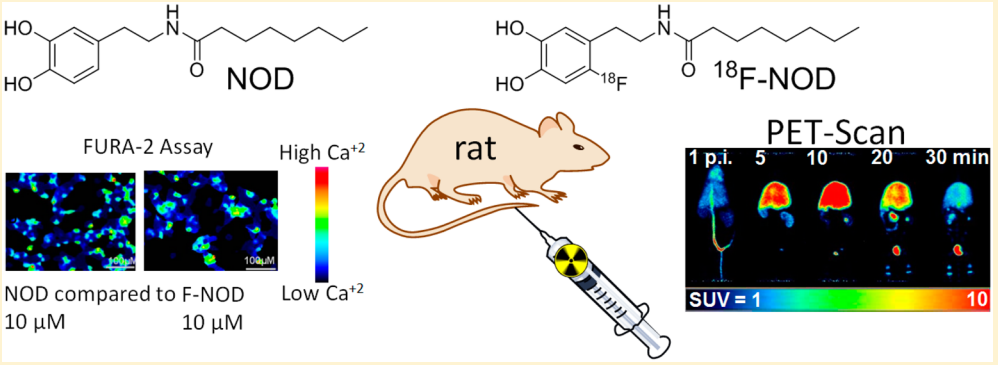

ABSTRACT: To mitigate pretransplantation injury in organs of potential donors, *N*-octanoyl dopamine (NOD) treatment might be considered as it does not affect hemodynamic parameters in braindead (BD) donors. To better assess optimal NOD concentrations for donor treatment, we report on the fast and facile radiofluorination of the NOD-derivative [^{18}F]F-NOD [^{18}F]**5** for in vivo assessment of NOD's elimination kinetics by means of PET imaging. [^{18}F]**5** was synthesized in reproducibly high radiochemical yields and purity (>98%) as well as high specific activities (>20 GBq/µmol). Stability tests showed no decomposition of [^{18}F]**5** over a period of 120 min in rat plasma. In vitro, low cell association was found for [^{18}F]**5**, indicating no active transport mechanism into cells. In vivo, [^{18}F]**5** exhibited a fast blood clearance and a predominant hepatobiliary elimination. As these data suggest that also NOD might be cleared fast, further pharmacokinetic evaluation is warranted.

INTRODUCTION

Current evidence suggests that low dose dopamine treatment of braindead (BD) donors improves transplantation outcome in recipients of renal and heart allografts.[1] Although the salutary effect of donor dopamine treatment has not been completely delineated, it has been suggested that the hemodynamic properties of dopamine do not play an essential role herein.[2] In vitro studies have identified three putative mechanisms by which dopamine may convey its protective properties in transplantation settings. First, dopamine can protect cells against cold inflicted injury as tested in vitro on endothelial cells, renal epithelial cells, and cardiomyocytes.[3,4] Second, dopamine is able to activate the transcription factor Nrf2 which regulates the expression of the tissue protective protein Heme oxygenase 1 (HO-1).[5] Third, dopamine has anti-inflammatory properties, reflected by down regulation of adhesion molecules and chemokines.[5,6]

Even though both prospective and retrospective studies have advocated the use of dopamine in BD donors as a meaningful modality to improve transplantation outcome,[1a,b] it has not been implemented in general guidelines for donor management. Currently, dopamine is used in donor management to stabilize blood pressure, albeit in clinical practice (nor)-

Received: August 10, 2016
Published: October 12, 2016

DOI: 10.1021/acs.jmedchem.6b01191
J. Med. Chem. 2016, 59, 9855−9865

Scheme 1. Synthesis Pathway of the Nonradioactive Reference Compound 5

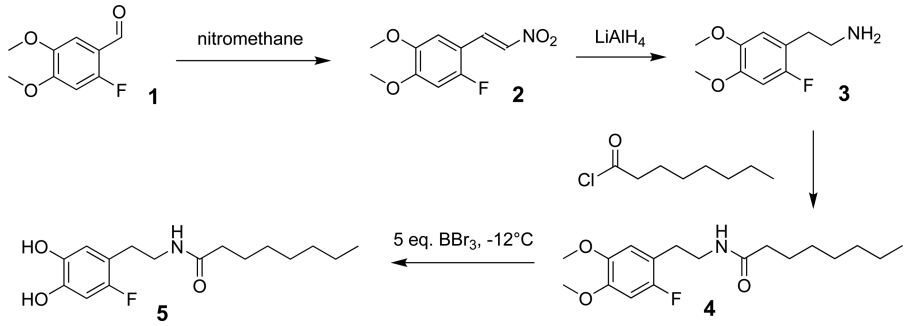

adrenaline is more frequently used for blood pressure stabilization of BD donors. In approximately 12% of treated donors, dopamine treatment needs to be discontinued as a consequence of tachycardia or hypertension. Moreover, the potential impact of inotropic agents on cardiomyocytes, i.e., increased cytosolic calcium concentration[7] and opening of the mitochondrial permeability transition pore,[8] may raise further concerns about the use of such agents in donor management.[9] This underscores the need for dopamine-like compounds that are devoid of hemodynamic action and yet have a similar or higher efficacy to protect organ allografts from pretransplantation injury. By N-acylation of dopamine, which largely abrogates adrenoceptor and dopaminergic receptor binding, a class of synthetic compounds was developed lacking hemodynamic actions while retaining the protective properties of dopamine.[1c,4b] As representative of *N*-acyl dopamines, we have shown that *N*-octanoyl dopamine (NOD) is superior to dopamine in vitro[10] and is highly effective in vivo to protect rat kidneys from ischemia-induced acute kidney injury (AKI).[11] The latter seems to be a consequence of the interaction with the transient receptor potential cation channel subfamily V member 1 (TRPV1),[12] as NOD was not renoprotective in TRPV1$^{-/-}$ rats.[13] Recently, it was also demonstrated that NOD treatment of BD donor rats reduced inflammation in the donor kidney and improved renal function when such grafts were transplanted into allogeneic recipients.[14]

Although these preclinical findings are promising, tissue distribution and pharmacokinetics of NOD have not been studied so far. As a first step we developed in the present study a NOD-based radiotracer to determine the in vivo tissue distribution and elimination kinetics of NOD by means of PET imaging.

In this work, we developed a fluorinated derivative of NOD, 2-fluoro-*N*-octanoyl dopamine **5** (F-NOD) and compared the in vitro behavior of F-NOD with NOD in various assays in order to determine whether F-NOD could act as an analogue to NOD. In brief, we compared the induction of HO-1, redoxactivity, TRPV1 activation, and EC_{50} of both compounds. Further, we performed a catechol *O*-methyl transferase (COMT) assay with NOD and F-NOD in order to investigate the cell intern metabolism. We developed a precursor **10** for radiofluorination in order to obtain the radiotracer [^{18}F]F-NOD. Next, we performed an in vitro cell assay with [^{18}F]F-NOD in human umbilical vein endothelial cells (HUVEC) for the determination of cell association. After this, we evaluated the in vivo behavior of radiolabeled [^{18}F]F-NOD in three Lewis rats.

RESULTS AND DISCUSSION

Synthesis of F-NOD. F-NOD was synthesized from 3,4-dimethoxy-2-fluorobenzaldehyde **1**, as outlined in Scheme 1. It was successfully converted to the β-nitrostyrene derivative **2** by the method of Milhazes et al.[15] To this end, nitromethane was used as solvent and ammonium acetate as base for generation of **2** (yield >81%), which was subsequently reduced with $LiAlH_4$ to the corresponding amine **3**. This was followed by introduction of an octanoyl group at the primary amine using octanoyl chloride in excess and selective removal of both methoxy groups with 5 equiv BBr_3 at −12 °C.[16]

In Vitro Studies with F-NOD and NOD. Several in vitro studies were conducted to test if F-NOD **5** displayed similar relevant biological properties as NOD **7**, i.e., inhibition of TNFα-mediated vascular cell adhesion molecule 1 (VCAM-1) expression, induction of HO-1, redox activity,[17] and the ability to activate TRPV1.[18] At higher concentrations, both NOD **7** and F-NOD **5** inhibited VCAM-1 expression almost to a similar extent, while at low concentrations, F-NOD **5** seemed to be less effective. This was more pronounced for induction of HO-1 (Figure 1A). We have previously demonstrated that the redox activity of NOD **7** is crucial for its ability to inhibit VCAM-1 expression.[19] In essence, this redox activity is provided by the ortho dihydroxy moiety on the benzene structure. Since these functional groups are also present in F-NOD **5**, this largely explains its ability to inhibit VCAM-1 expression and induce HO-1. We made use of a peroxidase-based luminol reaction to assess if a difference exists in the redox activity of the compounds. Dose−response experiments revealed highly significant effects of concentration ($F_{(15,559)}$ = 194.42, p < 0.001; two-way ANOVA, fixed effects) as well as of substance ($F_{(1,559)}$ = 26.78, p < 0.001). Although both NOD **7** and F-NOD **5** were able to completely quench chemiluminescence, for NOD **7** (EC_{50}: 12.12 μM), which was achieved at lower concentration as compared to F-NOD **5** (EC_{50}: 32.6 μM) (Figure 1B interaction: $F_{(15,559)}$ = 5.98, p < 0.001 two-way ANOVA, fixed effects). This suggests a small difference in redox activity between both compounds and might explain why F-NOD **5** is less efficiently inhibiting VCAM-1 and inducing HO-1 expression at low concentrations. In agreement with their redox activity, it was found that both compounds were able to protect endothelial cells against cold inflicted injury (Figure S1).

The TRPV1 activating properties were assessed in a heterologous cell assay. F-NOD **5**, like NOD **7**, was able to activate TRPV1 (Figure 2A). Dose−response experiments revealed highly significant effects of concentration ($F_{(11,137)}$ = 17.86, p < 0.001; two-way ANOVA, fixed effects) as well as of substance ($F_{(1,137)}$ = 12.38, p < 0.001). Thus, both substances

DOI: 10.1021/acs.jmedchem.6b01191
J. Med. Chem. 2016, 59, 9855−9865

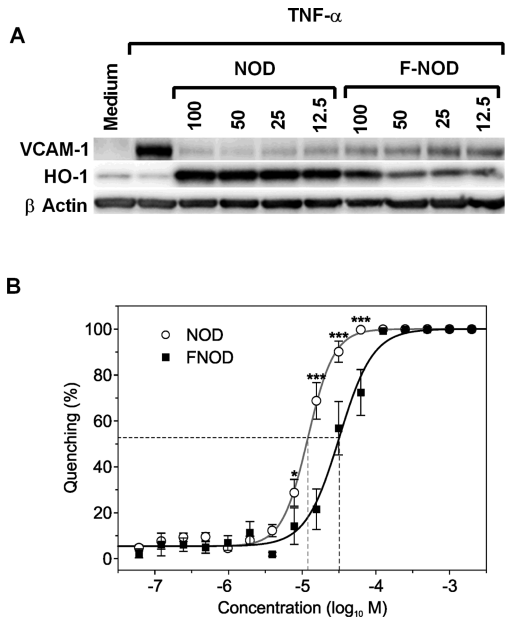

Figure 1. In vitro F-NOD **5** shows similar biological activity as NOD **7**: (A) Influence of F-NOD and NOD on TNFα-mediated VCAM-1 expression and induction of HO-1. Cells were stimulated overnight with TNFα 10 ng/mL in the presence of different concentrations of F-NOD **5** or NOD (0−100 μM). Cell lysates were prepared, and 15 μg of total protein was loaded on a 10% SDS PAGE. The gel was blotted and stained for VCAM-1 and HO-1. Equal loading of protein was confirmed with β-Actin. Note that at higher concentrations, inhibition of VCAM-1 and induction of HO-1 are comparable but not at lower concentrations to NOD in terms of its anti-inflammatory properties. (B) Redox activity of NOD and F-NOD: F-NOD **5** and NOD **7** showed comparable ability to quench luminescence in the luminol assay. Serial dilutions of NOD **7** or F-NOD **5** were added to 100 μL of reaction mixture containing 0.005 U of horseradish peroxidase (HRP), 2.5 mM luminol, and 0.9 mM *p*-coumaric acid. Chemiluminescence was measured directly after addition of 0.03% H_2O_2. The ability to quench peroxidase-mediated chemiluminescence was tested, and results are expressed as relative to the control to which neither NOD nor F-NOD were added along with ± SEM of all measurements. For each concentration and for each compound at least three independent measurements were performed. EC_{50} of NOD **7** was determined to be 12.12 μM and EC_{50} of F-NOD **5** 32.60 μM indicated by dashed lines, $^*p < 0.05$, $^{***}p < 0.001$ ANOVA with LSD post-hoc test.

were able to activate TRPV1 in a concentration-dependent manner, but NOD (EC_{50} = 7.10 μM [−5.15 ± 0.08]) was much more effective as compared to F-NOD (EC_{50} = 45.94 μM [−4.34 ± 0.12]) (Figure 2B).

It was further investigated, via computational molecular modeling, whether F-NOD also interacts with the TRPV1 binding pocket in similar fashion as NOD. No differences in putative interactions with amino acids inside the TRPV1 binding pocket were found between NOD **7** and F-NOD **5** (Figure S2). The 6-fold increase in EC_{50} value of F-NOD for TRPV1 activation may be a result of the insertion of fluorine as substituent in the aromatic ring. There, the fluorine might exert a negative inductive (−I) effect, thereby reducing the negative charge density in the aromatic ring, which in turn may influence the ability of F-NOD to access the TRPV1 binding site.[20]

Radiochemistry. For radiolabeling purposes, we initially intended to synthesize the precursor **10** by introduction of a nitro group into NOD **7**, which can be substituted by [^{18}F]fluoride (Scheme 2). Although the synthesis of NOD **7** was successful,[21] the subsequent nitration step to generate precursor **10** failed under various conditions.[22] This was most likely due to the acidic conditions during the nitration, which caused the hydrolysis of the octanoyl group. Therefore, precursor **10** was synthesized from 5-nitrified dopamine **8**, which was subsequently reacted with an excess of octanoyl chloride in order to maximize the yield of **9** (Scheme 2). The *O*-octanoyl groups of **9** were removed selectively by NaOH.

The radiolabeling of precursor **10** (0.5−1.8 mg) was optimized, and various reaction conditions were tested (reaction temperature of 20−120 °C in CH_3CN, DMF, or DMSO (0.5−1.0 mL) for 20−60 min, using [^{18}F]KF/K2.2.2/K_2CO_3 (Table 1)). Scheme 3 depicts the best radiolabeling conditions, which comprised 1.5 mg **10** in 0.5 mL DMSO for 30 min reaction time at 120 °C (radiochemical yield (RCY) = 45% (decay corrected−d.c.) (Figure 3A); specific activity 21.9−34.5 GBq/μmol for [^{18}F]F-NOD [^{18}F]**5**). Purification was performed by SepPak C_{18} light cartridges resulting in a radiochemical purity (RCP) of >99% and an absolute amount of radiotracer of 880 MBq after 90 min (starting from 3.43 GBq [^{18}F]fluoride) (Figure 3B). The identity of the product was checked by comparison of retention times on HPLC and TLC with that of the reference compound **5**.

Radiolabeling with acetonitrile as solvent resulted in a comparable RCY (38%, d.c.) but also in the formation of a lipophilic side product (>29%). Removal of this side product was only possible by semipreparative HPLC which ended in prolonged overall synthesis time and lower product activity. Radiolabeling utilizing DMF resulted in much lower RCY (6%, d.c.) (Table 1).

Lipophilicity and in Vitro Stability Tests of [^{18}F]F-NOD. The lipophilicity of a pharmacologically active compound is a fundamental physicochemical parameter. Hence, log *P*/log *D* determinations are of utmost importance and relevance to evaluate structure−activity relationships in medicinal chemistry as well as in radiopharmacy.[23] The lipophilicity (log *D*) of [^{18}F]**5** was determined at pH 7.5 to be 3.35 ± 0.04 (n = 3) using PBS and *n*-octanol according to the shake-flask method (OECD guideline).[24] Next, the stability of [^{18}F]**5** was evaluated in vitro. To this end, a solution of [^{18}F]**5** in PBS/3% EtOH (100 μL) was incubated with rat plasma (200 μL) and shaken for at least 120 min at 37 °C. Radio-TLC as well as radio-HPLC analyses were performed after 30, 60, and 120 min, respectively, and showed no decomposition or radiodefluorination of [^{18}F]**5** (RCP ≥ 98%) in the supernatant fraction, which showed a recovery rate of [^{18}F]**5** of 77−85% after protein precipitation of the incubation solution (100 μL) with acetonitrile (100 μL) at 0 °C. The precipitate contained 15−23% of the remained activity.

Cell Uptake and Stability Studies. Cell uptake studies were performed with HUVEC to assess to what extent [^{18}F]**5** is taken up by the cells, and if so, whether it is further metabolized. As depicted in Figure 4A, [^{18}F]**5** cell associated activity was approximately 0.14−0.21% of the applied dose (ID) after 120 min of incubation at 37 °C. HPLC analysis of the cell lysate extracts revealed only one radioactive peak at t_R = 4.07 min, corresponding to the intact [^{18}F]**5**, indicating that [^{18}F]**5** was not metabolized intracellularly within the time frame of the experiment.

In order to investigate the stability of [^{18}F]**5** in more detail, a catechol *O*-methyl transferase[25] (COMT) assay was performed[26] to assess if [^{18}F]**5** is a genuine substrate for

DOI: 10.1021/acs.jmedchem.6b01191
J. Med. Chem. 2016, 59, 9855−9865

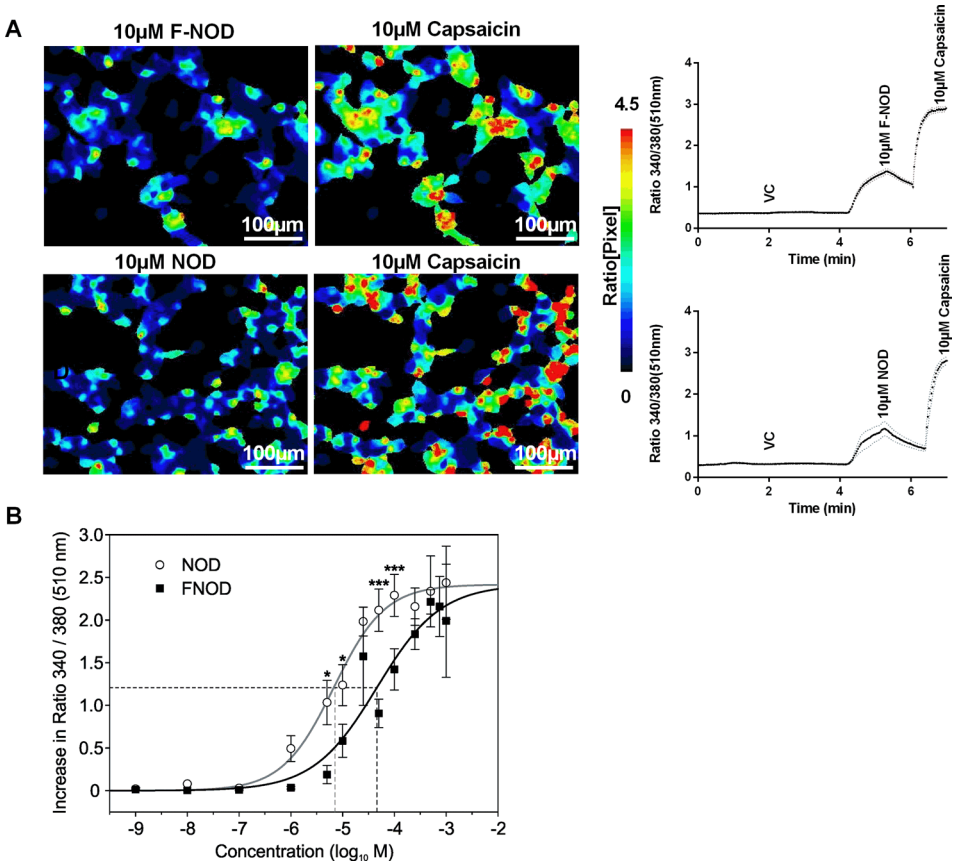

Figure 2. TRPV1 activation by F-NOD and NOD: (A) Representative images of a calcium imaging experiment using rTRPV1 transfected HEK293 cells (left panel). The ratio 340/380 at 510 nm—a measure proportional to free intracellular calcium—is false color coded, where warmer colors indicate increasing calcium values. Average time course traces are shown on the right panel. Cells were first either stimulated with 10 μM NOD **7** or 10 μM of F-NOD **5**, followed by 10 μM capsaicin to select rTRPV1 transfected cells and to see maximum response after washing away of the first substance; (B) rTRPV1 transfected HEK293 cells were stimulated with different concentrations of NOD **7** or F-NOD **5**: For each concentration and for each compound at least three independent measurements were performed. The results are expressed as average ratio 340/380 at 510 nm ± SEM of all measurements (n = 3−13). EC_{50} of F-NOD **5** was determined to be 45.94 μM and EC_{50} of NOD **7** 7.10 μM; EC_{50} values (NOD **7**: 7.10 μM and F-NOD **5**: 45.94 μM) indicated by dashed lines, *p < 0.05, ***p < 0.001 ANOVA with LSD post-hoc test.

Scheme 2. Synthesis Pathway Towards the Precursor 10

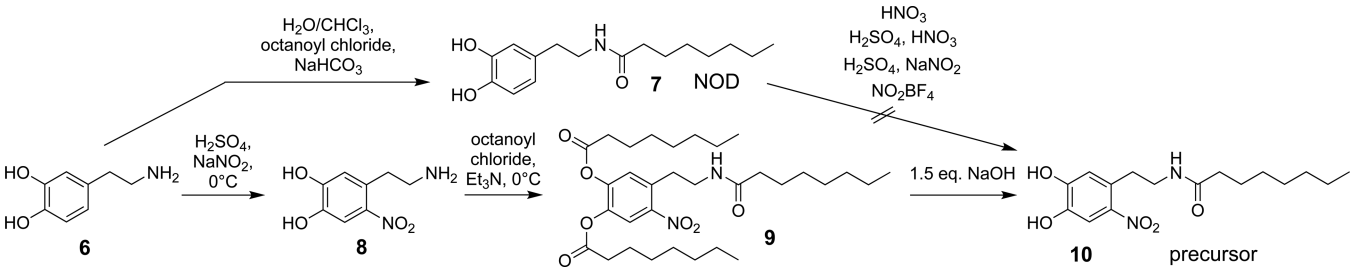

COMT. COMT is a ubiquitous intracellular enzyme that deactivates catechols by addition of a methyl group to one of the hydroxyl groups.[27] The assay was optimized using dopamine as gold standard, which is converted to 3-methoxythyramine (3-MT) (**11**) (Scheme 4).

Because of the high lipophilicity of both NOD and F-NOD, 10 μL of Tween20 was added, and higher concentrations of the methyl donor *S*-adenosyl-L-methionine (SAM) and COMT were used with prolonged reaction times (120−240 min) in order to allow the formation of 3-MNOD **12** and $(OMe)_2$-F-NOD **4**. Figure 4 displays the HPLC chromatograms of combined injections of different NOD and F-NOD derivatives (Figure 4 B,D) and the performed COMT assay (Figure 4 C,E) at different time points.

The conversion to the methylated derivatives proceeded slower in comparison to dopamine, which was totally converted to 3-MT after 120 min using low concentration of SAM and COMT. Methylation of NOD and F-NOD occurred at both hydroxy groups, resulting in double methylated derivatives. The rate of conversion to the methylated derivatives of F-NOD was slightly faster in comparison to NOD (see chromatograms C and E at 180 min in Figure 4). This might be explained by the strong negative inductive effect of the fluorine.

In Vivo Evaluation of [^{18}F]5. For assessment of the elimination kinetics of [^{18}F]**5** in three Lewis rats, different

DOI: 10.1021/acs.jmedchem.6b01191
J. Med. Chem. 2016, 59, 9855−9865

Table 1. Optimization of the Radiolabeling of Precursor 10 Regarding Reaction Time, Temperature, Solvent and Concentration of Precursor

amount of **10** [mg]	solvent	volume [mL]	temperature [°C]	labeling time [min]	RCY [%][a]	RCP [%] of crude [^{18}F]**5**
1.5	MeCN	0.5	20	30	10	25
1.5	MeCN	0.5	100	10	19	42
1.8	MeCN	0.5	100	40	18	55
1.8	MeCN	1.0	100	60	38	61
1.5	DMF	0.5	100	40	6	65
0.5	DMSO	0.5	110	40	16	83
1.5	DMSO	0.5	100	40	33	58
1.5	DMSO	0.5	120	30	45	69

[a]Unless otherwise stated, RCYs are all corrected for decay.

amounts of activity (4.8, 5.9, and 13.2 MBq) were injected to find the optimal dose for PET imaging, which was found to be 13.2 MBq. Elimination of [^{18}F]**5** was characterized by a fast blood clearance and substantial renal and hepatobiliary elimination (Figure 5A) being comparable with other lipophilic radiotracers.[28] The activity is flowing through the kidneys, peaking between 5 and 10 min (SUV_{bw} = 8 ± 5 g/mL) and being subsequently reallocated from the renal pelvis into the bladder within 30 min. Most of the injected activity accumulated in the liver as early as 8 min p.i. (SUV_{bw} = 21 ± 10 g/mL), possibly because of the lipophilic nature of [^{18}F]**5**. It seems probable that a substantial oxidative defluorination[29] of [^{18}F]**5** occurs in the liver by rat specific dehalogenase,[30] as reflected by a gradual accumulation of activity in bones starting at 60 min. After 120 min, most of the activity was found in the bladder (SUV_{bw} = 38.5 g/mL) and bones (SUV_{bw} = 9.8 g/mL). Time−activity curves for different organs are given in Figure 5B. The activity remains at a certain level (SUV_{bw} = 8 g/mL) within the renal pelvis and slowly eliminates into the bladder after 30 min. The liver activity is higher but also shows a faster elimination than from the renal pelvis without formation of a plateau.

CONCLUSION

In summary, we compared the in vitro behavior of F-NOD **5** and NOD **7** in various assays in order to determine whether F-NOD **5** could act as an analogue to NOD **7**. The results of F-NOD compared to NOD were similar with regard to induction of HO-1, redoxactivity, TRPV1 activation, and EC_{50}. NOD and F-NOD are both substrates for COMT. At both derivatives O-methylation takes place, but in comparison to dopamine, NOD and F-NOD exhibit a higher stability. This might be due to the higher lipophilicity of **5** and **7**, which hinders the O-methylation by the enzyme.

These data suggest that the radiolabeled [^{18}F]F-NOD could act as a tool for further determination of the in vivo behavior of NOD. In vitro cell assays with [^{18}F]F-NOD at HUVEC revealed low cell association (0.14−0.21%), which means that there is no active transport mechanism into the cell. The cell experiment suggests that the concentration of NOD must be at least 500 times higher outside the cell in order to achieve a certain concentration inside the cell after 2 h.

The in vivo experiments revealed a fast renal and hepatobiliary clearance of [^{18}F]F-NOD. Since the concentration of the radiotracer is very low, the metabolism of such small doses can be faster in comparison to a higher concentration of nonradioactive NOD given therapeutically. Due to the fast clearance it is recommended to use a high concentration of NOD as bolus injection or semihigh concentration via continuous injection in order to reach a renoprotective level in the kidneys for transplantation purposes.

In conclusion, we herein report on the fast and facile radiofluorination of the NOD-derivative [^{18}F]F-NOD [^{18}F]**5** for in vivo assessment of NOD's elimination kinetics by means of PET imaging. We demonstrated that F-NOD **5** and NOD **7** behave similarly in different in vitro assays and that both are substrates for COMT. [^{18}F]**5** was synthesized in reproducibly high radiochemical yields and purity (>98%) as well as high specific activities (>20 GBq/μmol). After a synthesis time of approximately 90 min, the radiotracer was ready for injection. Stability tests showed no decomposition of [^{18}F]**5** over a period of 120 min in rat plasma. Fast blood clearance and a predominant elimination by liver and kidneys were found for [^{18}F]**5** in vivo. Although these data suggest that also NOD **7** might be subject to a fast clearance, further in vivo pharmacokinetic evaluation is warranted. However, [^{18}F]**5** is useful for studying pharmacokinetics via biodistribution within a period of up to 30 min, due to the fast renal and hepatobiliary elimination and degradation in vivo between 30−60 min. [^{18}F]**5** might not be suitable for elongated pharmacokinetic and biodistribution studies in rodents, as it likely underlies an oxidative defluorination after 60 min.

EXPERIMENTAL SECTION

General procedures. All reagents and solvents were purchased from commercial suppliers and were used without further purification unless otherwise specified. NMR spectra were recorded on a 300 MHz Varian Mercury Plus and a 500 MHz Varian NMR System spectrometer (Palo Alto, CA). Chemical shifts (δ) are given in ppm and are referenced to the residual solvent resonance signals relative to $(CH_3)_4Si$ (^{1}H, ^{13}C) and the internal standard $CFCl_3$ (^{19}F). Mass spectra were obtained on a Bruker Daltonics microflex MALDI-TOF mass spectrometer (Bremen, Germany). Preparative column chromatography was performed on Merck silica gel 60. Reactions were monitored by thin-layer chromatography (TLC) on Merck silica gel F254 aluminum plates, with visualization under UV (λ = 254 nm) or by ninhydrin staining. If necessary, the purity was determined by high-performance liquid chromatography (HPLC). Purity of all final compounds was 95% or higher. Analytical (radio-)HPLC was performed on a Dionex UltiMate 3000 HPLC system (Thermo Scientific, Dreieich, Germany), equipped with a reverse-phase column (Merck Chromolith RP-18e; 100 × 4.6 mm plus a guard column 10 × 4.6 mm), a UV-diode array detector (210 nm, 254 nm), and a scintillation radiodetector Gabi Star (Raytest, Straubenhardt, Germany). The solvent system used was a gradient of acetonitrile:water (containing 0.1% TFA) (0−8 min: 0−100% MeCN) at a flow rate of 4

Scheme 3. Radiosynthesis Scheme of Radiotracer [^{18}F]F-NOD ([^{18}F]5)

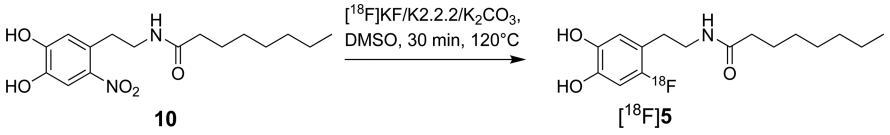

10 [^{18}F]**5**

DOI: 10.1021/acs.jmedchem.6b01191
J. Med. Chem. 2016, 59, 9855−9865

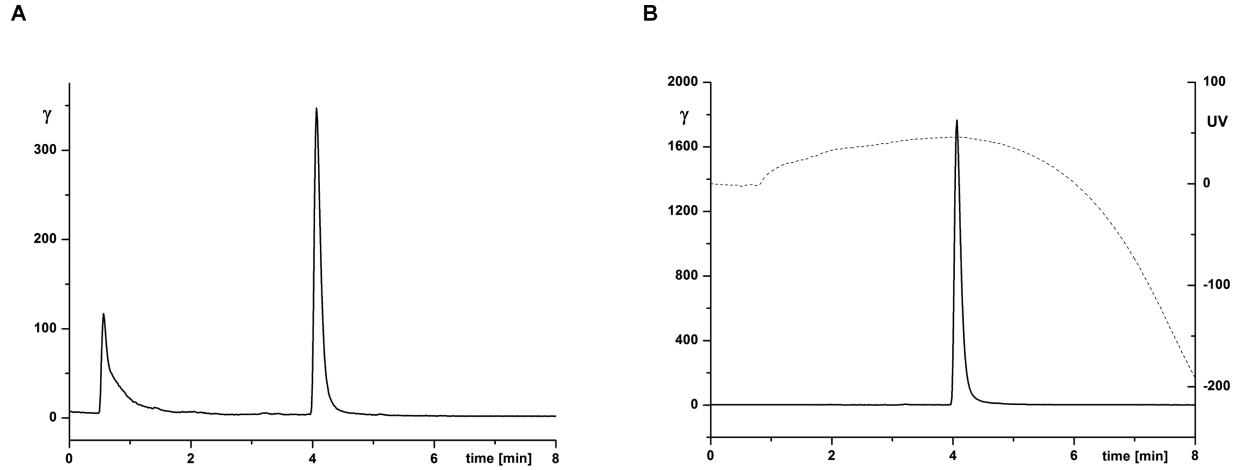

Figure 3. Synthesis and purification of [^{18}F]F-NOD: (A) Representative chromatogram of the crude radiolabeling reaction mixture and ^{18}F-incorporation (t_R = 0.65 min) into [^{18}F]F-NOD (t_R = 4.07 min) after 30 min at 120 °C in DMSO. (B) Representative analytical UV and radio-HPLC chromatograms of [^{18}F]F-NOD (t_R = 4.07 min) after purification via a SepPak C_{18} light cartridge: γ-trace (thick line) is depicting the radiochemical purity >99%, and UV-trace at 210 nm (dashed line) is depicting the chemical purity >96%.

mL/min unless otherwise stated. All radioactive compounds were identified using analytical radio-HPLC by comparison of the retention time of the reference compound and also by co-injection with the reference substance. A difference of 0.11 min between UV and γ-trace occurs as a result of the HPLC detector setup. Decay-corrected RCYs were quantified by calculation from QMA-eluted activity against C_{18}-eluted activity with respect to the purity of the final product in radio-HPLC and radio-TLC using a radio-TLC scanner (BAS-2500, Raytest). Cartridge purification was performed with Waters C_{18} light cartridges. [^{18}F]Fluoride was purchased from ZAG Zyklotron AG (Karlsruhe, Germany).

Cell Culture. HUVEC were isolated from the freshly available umbilical cord. Cells were grown in basal endothelial cell growth medium (Provitro GmbH, Berlin, Germany), supplemented with 2% fetal bovine serum and antibiotics. Cultures were maintained at 37 °C in a 5% CO_2 humidified atmosphere, and experiments were conducted on cells at approximately 80−90% confluence. HEK293 cells were cultured in T25 cm^2 flask with DMEM supplemented with 10% FCS, 1% penicillin streptomycin at 37 °C in 5% CO_2 humidified atmosphere.

Calcium Imaging and Data Analysis. HEK293 cells were seeded on 15 mm round glass coverslips in 12 well plates. 24 h post-plating, cells were transfected with rTRPV1 using metafectane (metafectene pro - Biontex Laboratories GmbH, Germany). 48 h post-transfection, cells were transferred into extracellular solution containing 137.6 mM NaCl, 5.4 mM KCl, 0.5 mM MgCl, 1.8 mM $CaCl_2$, 5 mM glucose, and 10 mM HEPES (Roth, Karlsruhe, Germany), loaded with the fluorescent dye FURA-2AM (1 μM; Biotrend, Cologne, Germany). Fluorescence was measured using an inverted microscope (IX-81 with Cell^R, Olympus, Hamburg, Germany) and an ORCA-R2 CCD camera (Hamamatsu Corp., Bridgewater, NJ, U.S.A.). After alternating excitation with light of 340 and 380 nm wavelength, the ratio of the fluorescence emission intensities at 510 nm (340 nm/380 nm [510 nm]) was calculated and digitized at 0.5 Hz. This fluorescence ratio is a relative measure of intracellular calcium concentration.[31] Analysis was done using Cell^R software (Olympus). All the cells that responded to capsaicin were taken as region of interest, and each coverslip was taken as an independent experiment. To determine the absolute change in ratio, the baseline value was subtracted from the peak. The data were analyzed using 2-way ANOVA with fixed effects for substance and concentration (STATISTICA Vs. 4.5, StatSoft, Inc.). LSD post-hoc test was used to identify substance differences at a given concentration.

Protein Isolation and Western Blotting. HUVEC cell lysates were generated by lysing in lysis buffer consisting of 10 mM Tris-HCl, 150 mM NaCl, 5 mM EDTA, 1% Triton X-100, 0.5% sodium deoxycholate, 1 μM dithiothreitol (DTT), proteinase inhibitor cocktail, and phosphatase inhibitor. Protein concentration was measured using Coomassie-Reagent (Pierce, Rockford, U.S.A.). Samples (15 μg protein extract) were heated to 95 °C for 5 min, loaded, and separated on 10% SDS-polyacrylamide gels followed by semidry blotted onto PVDF membranes (Roche, Mannheim, Germany). The membranes were incubated with 5% w/v nonfat dry milk in TBS/Tween 0.5% to block unspecific background staining and hereafter incubated overnight at 4 °C with anti-VCAM-1- (AF643, R&D Systems, Wiesbaden, Germany) or anti-HO-1-antibodies (ADI-SPA-895, Enzo, Biochem Inc., U.S.A.). Subsequently, the membranes were thoroughly washed with TBS-Tween 0.1% and incubated with the appropriate HRP conjugated secondary antibody, followed by five wash steps in TBS/Tween 0.1%. Proteins were visualized using enhanced chemiluminescence technology, according to the manufacturer's instructions (Pierce, Rockford, IL, U.S.A.). To confirm equal protein loading, membranes were stripped and reprobed with monoclonal anti-β-actin antibody (clone AC-74, ascites fluid, Sigma-Aldrich, U.S.A.).

Luminol Assay. The redox activity of the NOD and F-NOD was measured using luminol assay. Serial dilutions of the compounds were prepared in distilled water and added to luminol reaction mix (luminol 2.5 mM, *p*-coumaric acid 0.9 mM, and 0.3% H_2O_2). HRP (0.1 μg/μL) was added to the reaction mix, and quenching of chemiluminescence was measured immediately using infinite 200 PRO−Tecan microplate reader. The measurements were performed in triplicates.

COMT Assay (for Hydrophilic Substrate - Dopamine). The assay is performed with manufacturer specifications. In brief, the assay solution consists of 1 mM SAM in 100 μL of 20 mM tracepure HCl mixed with 100 μL of 10 mM $MgCl_2$ in tracepure water and 100 μL of 5 mM dithiothreitol in tracepure water and 200 μL of 0.5 M Tris buffer (pH 8.0 at 37 °C). The substrate (10 mM dopamine) is added in 200 μL tracepure water. 100 μL of this assay solution was mixed with 100 μL freshly prepared COMT solution (10 units) in 1% bovine serum albumin (BSA) and incubated at 37 °C for 1 h. Afterward, 100 μL of HCl conc. was added, and the mixture was cooled on ice for 5 min and centrifuged, and the supernatant was analyzed with analytical HPLC.

COMT Assay (for Hydrophobic Substrate). The assay solution consists of 100 μL of 10 mM $MgCl_2$ in tracepure water and 100 μL of 5 mM dithiothreitol in tracepure water and 500 μL of 0.5 M Tris buffer (pH 8.0 at 37 °C). 100 μL of this assay solution was mixed with 10 μL Tween20 and 20 μL of 14.6 mM SAM (300 nmol). Three μL (300 nmol) of the substrate (100 mM NOD or F-NOD in EtOH) is added, and finally 100 μL freshly prepared COMT-solution (75 units) in 1% BSA is added. The assay mixture is incubated at 37 °C for 2−4 h. Afterward, the mixture was cooled on ice for 5 min and centrifuged,

DOI: 10.1021/acs.jmedchem.6b01191
J. Med. Chem. 2016, 59, 9855−9865

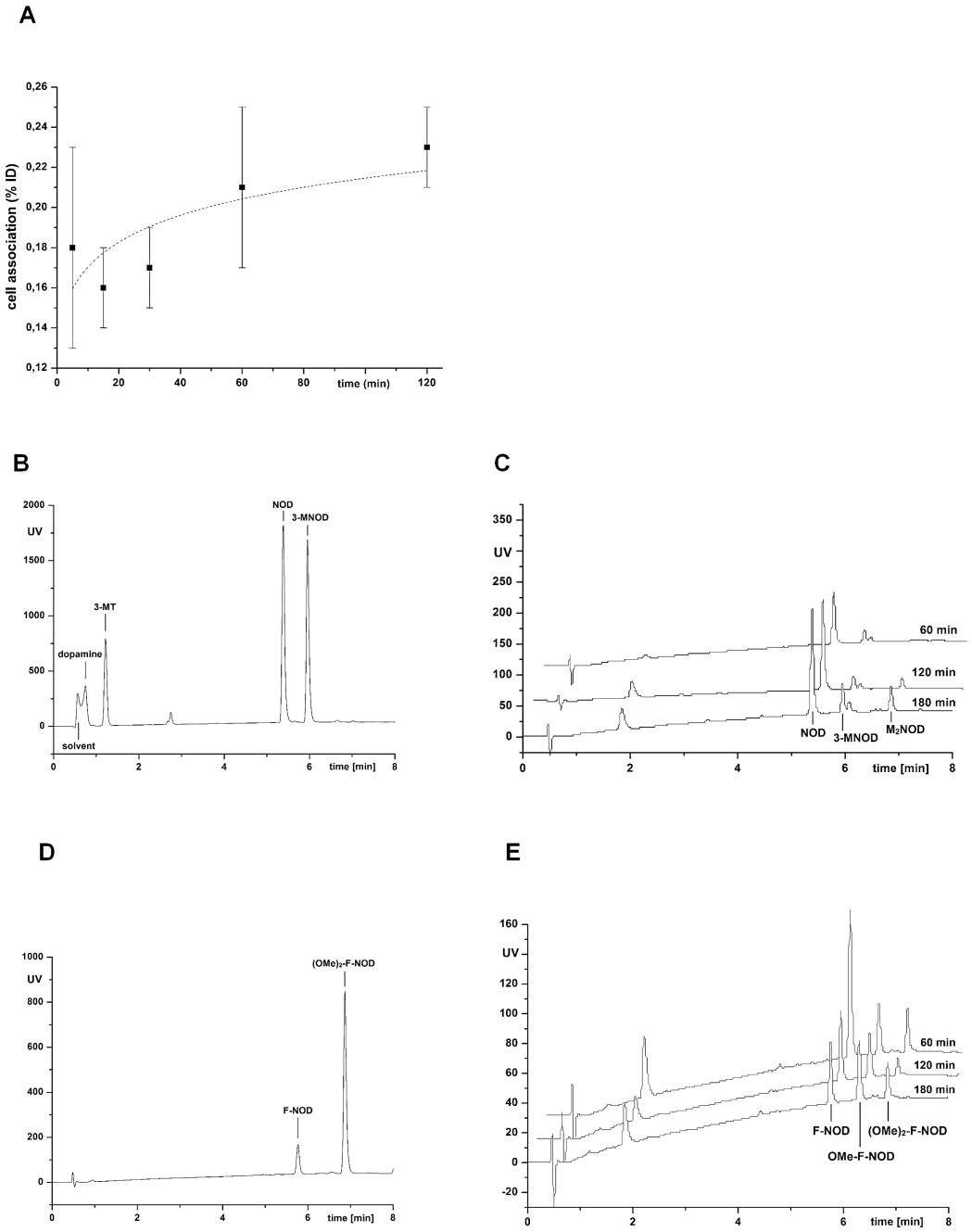

Figure 4. (A) Uptake of [^{18}F]**5** by endothelial cells over a period of 120 min at 37 °C (values represent means ± SD of three independent experiments). Representative chromatograms of: (B) NOD and its derivatives; (C) COMT assay for NOD, indicating a new, more lipophilic peak (16%) at the same retention time as 3-O-methoxy *N*-octanoyl dopamine **12**; (D) F-NOD and its methylated derivative; and (E) COMT assay for F-NOD. HPLC conditions: 0−50% MeCN + 0.1% TFA within 8 min.

Scheme 4. Synthesis Pathway Towards the O-Methylated Metabolite 12 of NOD used as Reference in COMT Assay

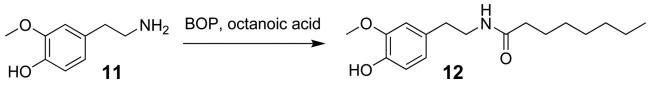

and the supernatant was extracted 3× with $CHCl_3$. The organic solvent is removed in vacuum, and the residue is dissolved in 1:1 MeCN/water and analyzed with analytical HPLC.

Cell Uptake Assay. Cells were incubated with ∼450 kBq [^{18}F]**5** per well on a six-well plate for different time points at 37 °C under normal atmosphere. For this purpose, 9.11 MBq [^{18}F]**5** was added to 20 mL cell medium and mixed, and 1 mL from that solution was added to every well containing cells. After incubation, the supernatant was collected, and the cells were washed three times with 1 mL PBS. The third washing solution was collected and finally 50 μL lysis buffer was added to the cells, and cells were scratched from the bottom of the well and collected for gamma counting.

Animal Experiments and Data Analysis. Lewis rats (LEW/Crl, Charles River Laboratories, Sulzfeld, Germany), aged 10 weeks and with a weight of 270−280 g, were employed for the initial PET experiments. The rats were anesthetized with isoflurane (2−2.5% delivered at 3.5 L/min), and a catheter was implanted in the V. femoralis for administration of the radiotracer. First experiments were set up as terminal experiments in order to assess the biodistribution after injection of different doses of [^{18}F]F-NOD (4.8, 5.9, and 13.2 MBq, in 0.9% NaCl solution, 150 μL, respectively).

DOI: 10.1021/acs.jmedchem.6b01191
J. Med. Chem. 2016, 59, 9855−9865

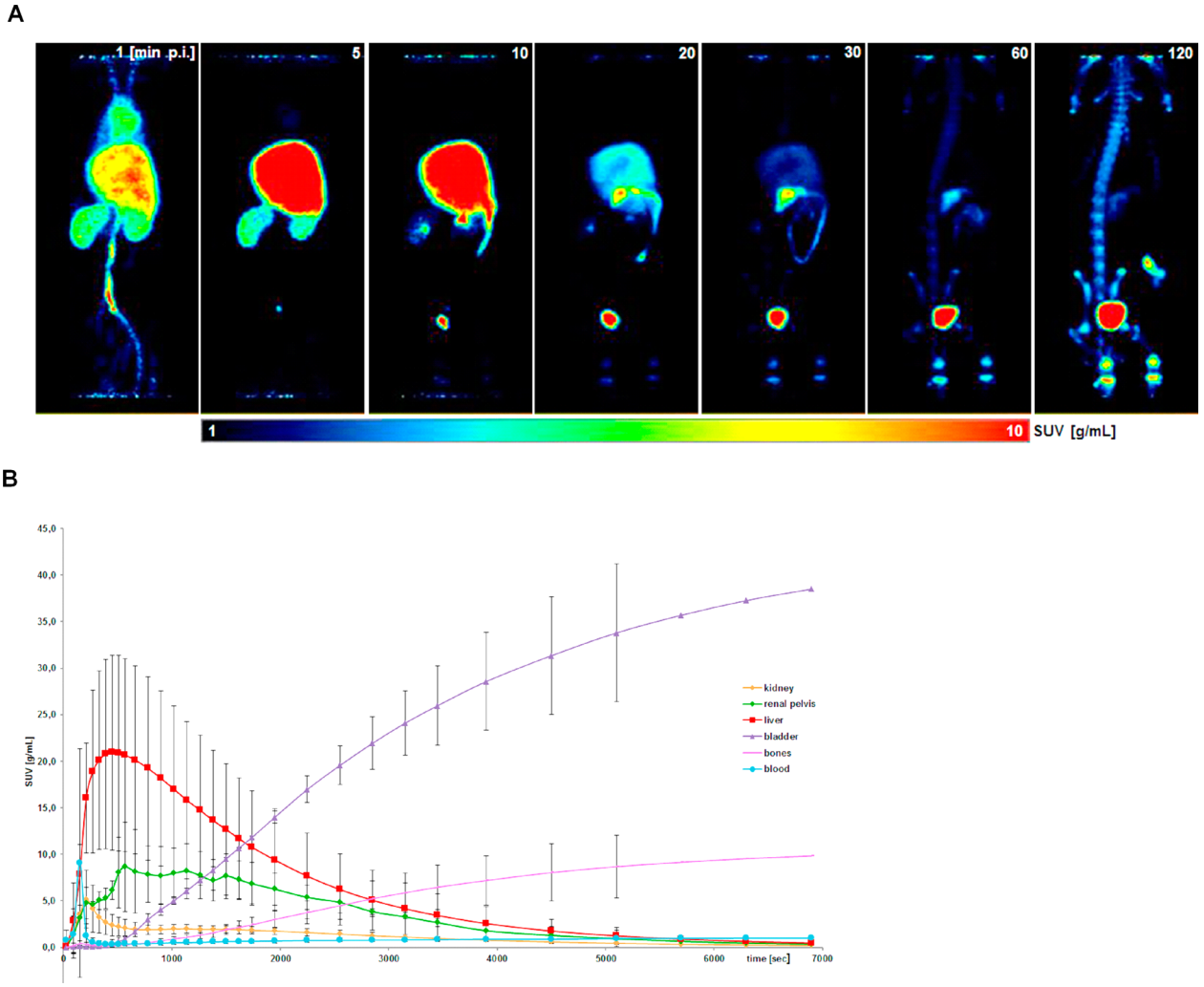

Figure 5. (A) PET images (maximal intensity projections) of Lewis rat injected with 13.2 MBq [^{18}F]**5**. (B) Time−activity curves showing the in vivo distribution of [^{18}F]**5** within 120 min (n = 3). Most of the activity accumulates in the liver. Some of the activity remains at a certain level inside the renal pelvis for 30 min.

All experiments were performed in compliance with the National Guidelines for Animal Protection, Germany, and the approval of the animal care committee. Small-animal PET experiments were conducted on an Albira PET System (Bruker Biospin MRI GmbH, Ettlingen, Germany). On injection of the radiotracer, a 120 min dynamic scan was initiated. The protocol comprised 31 frames (10 × 60, 10 × 120, 5 × 300, and 6 × 600 s). Reconstruction was performed using maximum likelihood expectation maximization (MLEM) algorithm with a matrix size of 20 × 20 and a pixel size of 0.5 mm (12 iterations) with the Albira Suite Reconstructor (Bruker Biospin MRI GmbH, Ettlingen, Germany) with the data output in kBq/cc. For data analysis, volumes of interests (VOI) were drawn in PMOD (version 3.608) to quantify the injected dose (PMOD Technologies Ltd., Zurich, Switzerland).

Materials. *(E)-1-Fluoro-4,5-dimethoxy-2-(2-nitrovinyl)benzene (**2**).* 3,4-Dimethoxy-2-fluorobenzaldehyde (**1**, 552 mg, 3.00 mmol) and ammonium acetate (58 mg, 0.75 mmol) were dissolved in nitromethane (5 mL), and the mixture was stirred at 80 °C for 6 h. After cooling to ambient temperature, excess nitromethane was removed and substituted by Et_2O. This solution was washed with water (2 × 10 mL) and dried with $MgSO_4$, and the yellow product (555 mg, 81%) was crystallized from a solution of Et_2O/petroleum ether (PE) 1:1. The purity of **2** was >97%, and the product was used without further purification. R_f = 0.47 (Et_2O:PE 1:1). ^{1}H NMR (500 MHz, $CDCl_3$): δ = 8.04 (d, $^3J_{H,H}$ = 13.7 Hz, 1H, -HC═CH-NO_2), 7.64 (d, $^3J_{H,H}$ = 13.7 Hz, 1H, -HC═CH-NO_2), 6.87 (d, $^4J_{H,F}$ = 6.7 Hz, 1H, H-6), 6.71 (d, $^3J_{H,F}$ = 11.7 Hz, 1H, H-3), 3.93 (s, 3H, 4-OCH_3), 3.90 ppm (s, 3H, 5-OCH_3). ^{13}C NMR (126 MHz, $CDCl_3$): δ = 157.6 (d, $^1J_{C,F}$ = 251.9 Hz, C-1), 153.7 (d, $^3J_{C,F}$ = 10.5 Hz, C-4), 146.0 (d, $^4J_{C,F}$ = 2.2 Hz, C-5), 137.1 (d, $^3J_{C,F}$ = 10.5 Hz, C-3), 132.6 (d, $^5J_{C,F}$ = 1.0 Hz, C═C-NO_2), 111.1 (d, $^4J_{C,F}$ = 4.4 Hz, C═C-NO_2), 100.5 (d, $^2J_{C,F}$ = 27.9 Hz, C-6), 56.5 ppm (2 × OCH_3). ^{19}F NMR (282 MHz, $CDCl_3$): δ = −114.6 ppm. MS (MALDI-TOF): m/z (%) 228 (30) [M + H]$^+$, 250 (30) [M + Na]$^+$. See Figure S3 for NMR signal assignment.

*2-(2-Fluoro-4,5-dimethoxyphenyl)ethan-1-amine (**3**).* To a solution of **2** (2.43 g, 10.69 mmol) in anhydrous THF (40 mL) under an N_2 atmosphere, a fresh solution of $LiAlH_4$ (1.02 g, 26.9 mmol) in THF (40 mL) was slowly added at 0 °C. The mixture was stirred for 15 min, and the reaction was quenched with ice-cold water. THF was removed under reduced pressure at 30 °C, brine was added, and the aqueous phase was extracted with ethyl acetate (EA) (3 × 50 mL). The organic phase was dried with $MgSO_4$, concentrated, and the crude product **3** was obtained as yellow oil (2.11 g, 99%). R_f = 0.16 (EE). ^{1}H NMR (300 MHz, $CDCl_3$): δ = 6.68 (d, $^4J_{H,F}$ = 7.1 Hz, 1H, H-6), 6.61 (d, $^3J_{H,F}$ = 11.0 Hz, 1H, H-3), 3.85 (s, 3H, 5-OCH_3), 3.84 (s, 3H, 4-OCH_3), 2.98 (t, ^3J = 6.1 Hz, 2H, NCH_2), 2.77 (t, ^3J = 6.9 Hz, 2H, CCH_2), 2.33 ppm (br s, 2H, NH_2). ^{13}C NMR (75 MHz, $CDCl_3$): δ = 155.2 (d, $^1J_{C,F}$ = 237.8 Hz, C-1), 148.4 (d, $^3J_{C,F}$ = 9.9 Hz, C-4), 145.1 (d, $^4J_{C,F}$ = 2.6 Hz, C-5), 116.2 (d, $^2J_{C,F}$ = 17.5 Hz, C-1), 113.3 (d, $^3J_{C,F}$ = 6.5 Hz, C-6), 100.2 (d, $^2J_{C,F}$ = 28.5 Hz, C-3), 56.5 (OCH_3), 56.1

DOI: 10.1021/acs.jmedchem.6b01191
J. Med. Chem. 2016, 59, 9855−9865

(OCH_3), 42.0 (NCH_2), 31.9 ppm (CCH_2). MS (MALDI-TOF): m/z (%) 223 (100) $[M + Na]^+$.

*N-(2-Fluoro-4,5-dimethoxyphenethyl)octanamide (**4**).* To a solution of **3** (2.07 g, 10.40 mmol) in CH_2Cl_2 (20 mL), a solution of octanoyl chloride (1.6 mL, 9.36 mmol) in CH_2Cl_2 (25 mL) was slowly added at 0 °C. To the resulting dark orange suspension Et_3N (2.2 mL, 15.6 mmol) was added, and the mixture was stirred for 15 min at 0 °C. The resulting pale yellow solution was washed with water and brine and dried with $MgSO_4$. The solvent was removed, and the crude product was purified by column chromatography (PE → PE:EA 10:1 → 5:1 → 4:1 → 1:1) to obtain compound **4** as pale yellow solid (1.41 g, 42%). R_f = 0.33 (PE:EA 1:2). Hot petroleum ether was used for recrystallization of **4**. ^{1}H NMR (500 MHz, DMSO-d_6): δ = 6.66 (t, $^4J_{H,F}$ = 7.1 Hz, 1H, H-6), 6.61 (d, $^3J_{H,F}$ =11.0 Hz, 1H, H-3), 5.49 (s, 1H, NH), 3.85 (s, 3H, OCH_3), 3.84 (s, 3H, OCH_3), 3.48 (dt, $^3J_{H,H}$ = 6.8 Hz, $^3J_{NH,H}$ = 6.1 Hz, 2H, NCH_2), 2.79 (t, ^3J = 6.9 Hz, 2H, CCH_2), 2.13 (t, ^3J = 7.6 Hz, 2H, H-α), 1.62−1.56 (m, 2H, H-β), 1.31−1.23 (m, 8H, H-γ,δ,ε,ζ), 0.89−0.86 ppm (m, 3H, CH_3). ^{13}C NMR (126 MHz, DMSO-d_6): δ = 173.2 (C═O), 155.1 (d, $^1J_{C,F}$ = 237.7 Hz, C-2), 148.4 (d, $^3J_{C,F}$ = 9.9 Hz, C-4), 145.2 (d, $^4J_{C,F}$ = 2.7 Hz, C-5), 116.1 (d, $^2J_{C,F}$ = 17.4 Hz, C-1), 113.0 (d, $^3J_{C,F}$ = 6.4 Hz, C-6), 100.1 (d, $^2J_{C,F}$ = 28.5 Hz, C-3), 56.4 (OCH_3), 56.4 (OCH_3), 39.7 (NCH_2), 36.9 (C-α) 31.7 (C-ε), 29.2 (C-γ), 29.0 (C-δ), 28.8 (C$\underline{C}H_2$), 25.7 (C-β), 22.6 (C-ζ), 14.1 ppm (CH_3). ^{19}F NMR (282 MHz, $CDCl_3$): δ = −126.1 ppm. MS (MALDI-TOF): m/z (%) 326 (100) $[M + H]^+$. Analytical HPLC: t_R = 4.54 min.

*N-(2-Fluoro-4,5-dihydroxyphenethyl)octanamide (**5**).* To a solution of **4** (734 mg, 2.26 mmol) in CH_2Cl_2 (100 mL), a solution of BBr_3 (11.3 mL, 11.3 mmol, 1 M) in CH_2Cl_2 was slowly added at −12 °C within 5 min. The mixture was stirred for 135 min at −10 °C and was allowed to reach ambient temperature for 60 min. Water (30 mL) was added to quench the reaction, and the mixture was extracted with CH_2Cl_2 (1×) and EA (2×). The combined organic phases were dried with $MgSO_4$ and concentrated under reduced pressure, and the crude product was purified by column chromatography (PE → PE:EA 1:1) to obtain compound **5** as pale yellow solid (602 mg, 90%). R_f = 0.44 (PE:EA 1:3), 0.85 (methanol). ^{1}H NMR (300 MHz, DMSO-d_6): δ = 9.09 (s, 1H, OH), 8.72 (s, 1H, OH), 7.81 (t, ^3J = 5.7 Hz, 1H, NH), 6.54 (d, $^4J_{H,F}$ = 7.8 Hz, 1H, H-6), 6.48 (d, $^3J_{H,F}$ = 10.9 Hz, 1H, H-3), 3.18−3.11 (m, 2H, NCH_2), 2.52 (t, ^3J = 7.3 Hz, 2H, CCH_2), 2.01 (t, ^3J = 7.2 Hz, 2H, H-α), 1.48−1.43 (m, 2H, H-β), 1.27−1.23 (m, 8H, H-γ,δ,ε,ζ), 0.88−0.83 ppm (m, 3H, CH_3). ^{13}C NMR (75 MHz, DMSO-d_6): δ = 171.9 (C═O), 153.3 (d, $^1J_{C,F}$ = 233.2 Hz, C-2), 144.2 (d, $^3J_{C,F}$ = 11.2 Hz, C-4), 141.3 (d, $^4J_{C,F}$ = 2.3 Hz, C-5), 116.5 (d, $^3J_{C,F}$ = 6.0 Hz, C-6), 115.0 (d, $^2J_{C,F}$ = 17.2 Hz, C-1), 102.8 (d, $^2J_{C,F}$ = 26.4 Hz, C-3), 39.0 (NCH_2), 35.3 (C-α) 31.1 (C-ε), 28.5 (C-γ), 28.4 (C-δ), 28.1 (C$\underline{C}H_2$), 25.2 (C-β), 22.0 (C-ζ), 13.9 ppm (CH_3). ^{19}F NMR (282 MHz, DMSO-d_6): δ = −129.7 ppm. MS (MALDI-TOF): m/z (%) 298 (100) $[M + H]^+$. Analytical HPLC: t_R = 3.96 min.

*4-(2-Aminoethyl)-5-nitrobenzene-1,2-diol (**8**).* 6-Nitrodopamine **8** was prepared according to the literature.[22d] In brief, to a solution of dopamine hydrochloride (1.50 g, 7.91 mmol) in water (45 mL) being cooled to 0 °C, $NaNO_2$ (1.89 g, 27.39 mmol) was added, and the mixture was stirred for 15 min. To the pale yellow solution, an ice-cold solution of 20% H_2SO_4 (3.5 mL) was slowly added. The yellow product starts to precipitate from the brown solution. The product was filtered, washed with cold water and methanol, and dried in high vacuum to obtain **8** as yellow solid (1.21 g, 77%). NMR and MS analyses were consistent with the literature.[22d]

*4-Nitro-5-(2-octanamidoethyl)-1,2-phenylene dioctanoate (**9**).* To a solution of **8** (500 mg, 2.52 mmol) in CH_2Cl_2 (10 mL), a solution of octanoyl chloride (1.19 mL, 6.98 mmol) in CH_2Cl_2 (3 mL) was slowly added at 0 °C. Et_3N (1.23 mL, 8.82 mmol) was added, and the mixture was stirred at ambient temperature for 16 h. CH_2Cl_2 was removed, and the residue was redissolved in EA (20 mL) and washed with brine. The organic phase was dried with Na_2SO_4 and concentrated under reduced pressure, and the crude product was purified by column chromatography (PE → PE:EA 5:1 → 3:1) to obtain compound **9** as pale yellow solid (431 mg, 33%). R_f = 0.59 (PE:EA 1:1). Hot acetonitrile was used for recrystallization of **9**. ^{1}H NMR (500 MHz, $CDCl_3$): δ = 7.89 (s, 1H, H-3), 7.21 (s, 1H, H-6), 5.79 (s, 1H, NH), 3.61−3.57 (dt, $^3J_{H,H}$ = 6.8 Hz, $^3J_{NH,H}$ = 6.4 Hz, 2H, NCH_2), 3.12 (t, ^3J = 6.8 Hz, 2H, CCH_2), 2.55 (t, ^3J = 7.5 Hz, 2H, 2-O(CO)CH_2), 2.54 (t, ^3J = 7.5 Hz, 2H, 1-O(CO)CH_2), 2.17 (t, ^3J = 7.7 Hz, 2H, N(CO)CH_2), 1.70−1.63 (m, 4H, O(CO)$CH_2C\underline{H}_2$), 1.56−1.50 (m, 2H, N(CO)$CH_2C\underline{H}_2$), 1.44−1.22 (m, 24H, 3xH-γ,δ,ε,ζ), 0.92−0.85 ppm (m, 9H, 3 × CH_3). ^{13}C NMR (126 MHz, $CDCl_3$): δ = 173.7 (NC═O), 170.5 (2-OC═O), 170.2 (1-OC═O), 146.0 (C-1), 145.8 (C-2), 140.9 (C-4), 133.2 (C-5), 127.5 (C-6), 120.9 (C-3), 39.7 (NCH_2), 36.6 (N−C-α), 34.0 (2-O-C-α), 33.9 (1-O-C-α), 32.8 (C$\underline{C}H_2$), 31.7 (N−C-ε), 31.6 (2 × O-C-ε), 29.0 (6 × C-γ,δ), 25.6 (N−C-β), 24.8 (2 × O-C-β), 22.6 (3 × C-ζ), 14.0 ppm (3 × CH_3). MS (MALDI-TOF): m/z (%) 577 (60) $[M + H]^+$. Analytical HPLC: t_R = 7.75 min.

*N-(4,5-Dihydroxy-2-nitrophenethyl)octanamide (**10**).* **9** (150 mg, 0.26 mmol) was dissolved in acetonitrile (25 mL) at 30 °C. The mixture was cooled to 0 °C, and a solution of 0.1 M NaOH (2.6 mL, 0.26 mmol) was added dropwise. The mixture was then stirred for 4 h at 50 °C. After this, water (20 mL) was added, and the mixture was extracted with EA (2×). The organic phase was dried with $MgSO_4$ and concentrated under reduced pressure, and the crude product was purified by column chromatography (PE → PE:EA 1:1) to obtain compound **10** as yellow solid (83 mg, 99%). R_f = 0.20 (PE:EA 1:1). ^{1}H NMR (500 MHz, DMSO-d_6): δ = 10.33 (s, 1H, OH), 9.81 (s, 1H, OH), 7.84 (t, ^3J = 5.7 Hz, 1H, NH), 7.48 (s, 1H, H-6), 6.68 (s, 1H, H-3), 3.27−3.23 (m, 2H, NCH_2), 2.88 (t, ^3J = 7.1 Hz, 2H, CCH_2), 1.99 (t, ^3J = 7.5 Hz, 2H, H-α), 1.47−1.41 (m, 2H, H-β), 1.28−1.17 (m, 8H, H-γ,δ,ε,ζ), 0.87−0.84 ppm (m, 3H, CH_3). ^{13}C NMR (126 MHz, DMSO-d_6): δ = 171.9 (C═O), 151.7 (C-5), 143.9 (C-4), 139.0 (C-2), 128.1 (C-1), 118.1 (C-6), 111.9 (C-3), 39.7 (NCH_2), 35.3 (C-α) 32.8 (C-ε), 31.0 (C$\underline{C}H_2$), 28.5 (C-γ), 28.3 (C-δ), 25.1 (C-β), 22.0 (C-ζ), 13.8 ppm (CH_3). MS (MALDI-TOF): m/z (%) 325 (100) $[M + H]^+$. Analytical HPLC: t_R = 4.06 min.

*N-(4-Hydroxy-3-methoxyphenethyl)octanamide (**12**).* 3-Methoxytyramine (3-MT) (50 mg, 0.25 mmol) was mixed with octanoic acid (40 μL, 0.25 mmol) and BOP (110 mg, 0.25 mmol) in 2 mL anhydrous THF. The solution was cooled to 0 °C, and Et_3N (105 μL, 0.75 mmol) dissolved in 400 μL THF was added dropwise within 15 min. The reaction was continued at ambient temperature for 16 h. THF was substituted by 10 mL Et_2O and the organic phase was washed 3× with HCl (3 mL, 1 M), 2× with $NaHCO_3$-solution (5 mL, 1 M), and 2× with brine (5 mL). The organic phase was dried with $MgSO_4$, and the product was recrystallized from Et_2O:hexane 1:1 to obtain a pale yellow solid (70 mg, 95%). R_f = 0.30 (PE:EE 1:2). ^{1}H NMR (500 MHz, $CDCl_3$): δ = 6.85 (d, ^3J = 7.9 Hz, 1H, H-2), 6.71−6.66 (m, 2H, H-5,6), 5.50 (s, 1H, NH), 3.88 (s, 3H, OCH_3), 3.49 (t, ^3J = 6.8 Hz, 2H, NCH_2), 2.74 (t, ^3J = 6.9 Hz, 2H, CCH_2), 2.21 (d, ^3J = 2.9 Hz, 1H, OH), 2.13 (t, ^3J = 7.6 Hz, 2H, (CO)CH_2), 1.63−1.54 (m, 2H, N(CO)$CH_2C\underline{H}_2$), 1.32−1.22 (m, 8H, H-γ,δ,ε,ζ), 0.89−0.86 ppm (m, 3H, CH_3). ^{13}C NMR (126 MHz, $CDCl_3$): δ = 173.1 (NC═O), 146.6 (C-3), 144.3 (C-4), 140.9 (C-1), 121.3 (C-6), 114.4 (C-5), 111.1 (C-2), 55.9 (OCH_3), 40.6 (NCH_2), 36.9 (C$\underline{C}H_2$), 35.4 (C-α), 31.7 (N−C-ε), 29.2 (C-γ), 29.0 (C-δ), 25.8 (C-β), 22.6 (C-ζ), 14.1 ppm (CH_3). MS (MALDI-TOF): m/z (%) 294 (70) $[M + H]^+$. Analytical HPLC: t_R = 6.13 min (0−8 min: 0−50% MeCN).

Radiochemistry. *N-(2-[^{18}F]Fluoro-4,5-dihydroxyphenethyl)-octanamide [^{18}F]**5**.* No-carrier-added aqueous [^{18}F]fluoride (3.43 GBq) was trapped on a Waters QMA cartridge, which was preconditioned with 1 M $NaHCO_3$ (5 mL) and tracepure H_2O (10 mL). [^{18}F]Fluoride was eluted with a freshly prepared Kryptofix-solution (12.5 mg K2.2.2, 800 μL MeCN, 200 μL tracepur H_2O, 10 μL 1 M K_2CO_3) into the reaction vessel and dried via azeotropic distillation under a gentle stream of helium (2 mL/min) at 100 °C for 4 min at 600 mbar, followed by addition of anhydrous acetonitrile (2 × 0.8 mL; 3 min at 600 mbar) and 4 min at full vacuum. Afterward, **10** (1.5 mg, 4.62 μmol) dissolved in anhydrous DMSO (500 μL) was added, and the reaction mixture was stirred at 120 °C for 30 min. Water (15 mL) was added, the solution was passed through a SepPak tC_{18} plus light cartridge (145 mg sorbent, preconditioned with 5 mL Et_2O), and the cartridge was washed with water (10 mL, cartridge kept

DOI: 10.1021/acs.jmedchem.6b01191
J. Med. Chem. 2016, 59, 9855−9865

wet), followed by elution of [^{18}F]**5** with diethyl ether (3 mL, the first yellow 1.1 mL were discarded until the eluted fraction was colorless). The solvent was evaporated at 80 °C at 900 mbar in a gentle stream of helium for 4−5 min to afford 880 MBq (RCY = 45%, d.c.) [^{18}F]**5** with a RCP of > 99% within approximately 90 min and with a specific activity of 28 ± 6 GBq/μmol (n = 5). Radio-HPLC: t_R = 4.07 min. Radio-TLC: R_f = 0.85 (methanol). For injection purposes, [^{18}F]**5** was redissolved in a suitable amount (0.4−1.0 mL) of 0.9% NaCl solution for injection +9% EtOH and purified by a sterile filter (0.22 μm) resulting in a final pH of 7.57 ± 0.3.

Ethical Statement. Umbilical cords for isolation of HUVEC were received from donors in the Department of Obstetrics and Gynecology, University Medical Center Mannheim, Heidelberg University, Heidelberg, Germany. This was approved by local ethics committee (Medizinische Ethikkommission II der Medizinischen Fakultät Mannheim), and all donors gave their written informed consent (ethic application no. 2015-518N-MA).

■ ASSOCIATED CONTENT

Supporting Information

The Supporting Information is available free of charge on the ACS Publications website at DOI: 10.1021/acs.jmedchem.6b01191.

Methods for cellular cold inflicted injury model, LDH assay, and computational molecular modeling (PDF)

Compound data (CSV)

■ AUTHOR INFORMATION

Corresponding Authors

*E-mail: Marc.Pretze@medma.uni-heidelberg.de; Phone: +49 (0)621 383 6045.

*E-mail: Bjoern.Waengler@medma.uni-heidelberg.de; Phone: +49 (0)621 383 5594.

Author Contributions

○These authors contributed equally.

Notes

The authors declare no competing financial interest.

■ ACKNOWLEDGMENTS

The excellent technical assistance of Ms. Anne-Maria Suhr in the animal experiments and of Ms. Handan Moerz in calcium imaging experiments is gratefully acknowledged. We would like to thank Tobias Timmermann for measuring the NMR spectra and Dr. Uwe Seibold for measuring the MALDI-MS spectra. The fundings "Perspektivförderung des Ministeriums für Wissenschaft und Kunst Baden-Württemberg" and "Albert und Anneliese Konanz-Stiftung - Hochschule Mannheim" are gratefully acknowledged.

■ ABBREVIATIONS USED

NOD, *N*-octanoyl dopamine; BD, braindead; TNF-α, tumor necrosis factor alpha; VCAM-1, vascular cell adhesion protein 1; TRPV1, transient receptor potential cation channel subfamily V member 1; AKI, acute kidney injury; CCR2, CC chemokine receptor 2; CCL2, CC chemokine ligand 2; CCR5, CC chemokine receptor 5; TLC, thin-layer chromatography

■ REFERENCES

(1) (a) Schnuelle, P.; Gottmann, U.; Höger, S.; Boesebeck, D.; Lauchart, W.; Weiss, C.; Fischereder, M.; Jauch, K.-W.; Heemann, U.; Zeier, M.; Hugo, C.; Pisarski, P.; Krämer, B. K.; Lopau, K.; Rahmel, A.; Benck, U.; Birck, R.; Yard, B. A. Effects of donor pretreatment with dopamine on graft function after kidney transplantation. *J. Am. Med. Assoc.* **2009**, *302*, 1067−1075. (b) Benck, U.; Hoeger, S.; Brinkkoetter, P. T.; Gottmann, U.; Doenmez, D.; Boesebeck, D.; Lauchart, W.; Gummert, J.; Karck, M.; Lehmkuhl, H. B.; Bittner, H. B.; Zuckermann, A.; Wagner, F.; Schulz, U.; Koch, A.; Bigdeli, A. K.; Bara, C.; Hirt, S.; Berchtold-Herz, M.; Brose, S.; Herold, U.; Boehm, J.; Welp, H.; Strecker, T.; Doesch, A.; Birck, R.; Krämer, B. K.; Yard, B. A.; Schnuelle, P. Effects of donor pre-treatment with dopamine on survival after heart transplantation: a cohort study of heart transplant recipients nested in a randomized controlled multicenter trial. *J. Am. Coll. Cardiol.* **2011**, *58*, 1768−1777. (c) Lösel, R. M.; Schnetzke, U.; Brinkkoetter, P. T.; Song, H.; Beck, G.; Schnuelle, P.; Höger, S.; Wehling, M.; Yard, B. A. N-octanoyl dopamine, a non-hemodyanic dopamine derivative, for cell protection during hypothermic organ preservation. *PLoS One* **2010**, *5*, e9713.

(2) (a) Hoeger, S.; Gottmann, U.; Liu, Z.; Schnuelle, P.; Birck, R.; Braun, C.; van der Woude, F. J.; Yard, B. A. Dopamine treatment in brain-dead rats mediates anti-inflammatory effects: the role of hemodynamic stabilization and D-receptor stimulation. *Transplant Int.* **2007**, *20*, 790−799. (b) Hoeger, S.; Reisenbuechler, A.; Gottmann, U.; Doyon, F.; Braun, C.; Kaya, Z.; Seelen, M. A.; van Son, W. J.; Waldherr, R.; Schnuelle, P.; Yard, B. A. Donor dopamine treatment in brain dead rats is associated with an improvement in renal function early after transplantation and a reduction in renal inflammation. *Transplant Int.* **2008**, *21*, 1072−1080.

(3) Kassmann, M.; Harteneck, C.; Zhu, Z.; Nurnberg, B.; Tepel, M.; Gollasch, M. Transient receptor potential vanilloid 1 (TRPV1), TRPV4, and the kidney. *Acta Physiol.* **2013**, *207*, 546−564.

(4) (a) Yard, B.; Beck, G.; Schnuelle, P.; Braun, C.; Schaub, M.; Bechtler, M.; Gottmann, U.; Xiao, Y.; Breedijk, A.; Wandschneider, S.; Lösel, R.; Sponer, G.; Wehling, M.; van der Woude, F. J. Prevention of cold-preservation injury of cultured endothelial cells by catecholamines and related compounds. *Am. J. Transplant.* **2004**, *4*, 22−30. (b) Vettel, C.; Hottenrott, M. C.; Spindler, R.; Benck, U.; Schnuelle, P.; Tsagogiorgas, C.; Krämer, B. K.; Hoeger, S.; El-Armouche, A.; Wieland, T.; Yard, B. A. Dopamine and lipophilic derivates protect cardiomyocytes against cold preservation injury. *J. Pharmacol. Exp. Ther.* **2014**, *348*, 77−85.

(5) Berger, S. P.; Hünger, M.; Yard, B. A.; Schnuelle, P.; van der Woude, F. J. Dopamine induces the expression of heme oxygenase-1 by human endothelial cells in vitro. *Kidney Int.* **2000**, *58*, 2314−2319.

(6) (a) Beck, G.; Brinkkoetter, P.; Hanusch, C.; Schulte, J.; van Ackern, K.; van der Woude, F. J.; Yard, B. A. Clinical review: immunomodulatory effects of dopamine in general inflammation. *Crit. Care* **2004**, *8*, 485−491. (b) Kapper, S.; Beck, G.; Riedel, S.; Prem, K.; Haak, M.; van der Woude, F. J.; Yard, B. A. Modulation of chemokine production and expression of adhesion molecules in renal tubular epithelial and endothelial cells by catecholamines. *Transplantation* **2002**, *74*, 253−260.

(7) (a) van der Heyden, M. A.; Wijnhoven, T. J.; Opthof, T. Molecular aspects of adrenergic modulation of cardiac L-type Ca2+ channels. *Cardiovasc. Res.* **2005**, *65*, 28−39. (b) Mann, D. L.; Kent, R. L.; Parsons, B.; Cooper, G. T. Adrenergic effects on the biology of the adult mammalian cardiocyte. *Circulation* **1992**, *85*, 790−804.

(8) (a) Halestrap, A. P.; Kerr, P. M.; Javadov, S.; Woodfield, K. Y. Elucidating the molecular mechanism of the permeability transition pore and its role in reperfusion injury of the heart. *Biochim. Biophys. Acta, Bioenerg.* **1998**, *1366*, 79−94. (b) Leung, A. W.; Halestrap, A. P. Recent progress in elucidating the molecular mechanism of the mitochondrial permeability transition pore. *Biochim. Biophys. Acta, Bioenerg.* **2008**, *1777*, 946−952.

(9) (a) Roy, N.; Friehs, I.; Cowan, D. B.; Zurakowski, D.; McGowan, F. X.; del Nido, P. J. Dopamine induces postischemic cardiomyocyte apoptosis in vivo: an effect ameliorated by propofol. *Ann. Thorac. Surg.* **2006**, *82*, 2192−2199. (b) Nixon, J. L.; Kfoury, A. G.; Brunisholz, K.; Horne, B. D.; Myrick, C.; Miller, D. V.; Budge, D.; Bader, F.; Everitt, M.; Saidi, A.; Stehlik, J.; Schmidt, T. C.; Alharethi, R. Impact of high-dose inotropic donor support on early myocardial necrosis and outcomes in cardiac transplantation. *Clin. Transplant.* **2012**, *26*, 322−327.

DOI: 10.1021/acs.jmedchem.6b01191
J. Med. Chem. 2016, 59, 9855−9865

(10) (a) Shashoua, V. E.; Hesse, G. W. N-docosahexaenoyl, 3-hydroxytyramine: A dopaminergic compound that penetrates the blood-brain barrier and suppresses appetite. *Life Sci.* **1996**, *58*, 1347−1357. (b) Liu, Z.; Hoeger, S.; Schnuelle, P.; Feng, Y.; Goettmann, U.; Waldherr, R.; van der Woude, F. J.; Yard, B. Donor dopamine pretreatment inhibits tubulitis in renal allografts subjected to prolonged cold preservation. *Transplantation* **2007**, *83*, 297−303.
(11) (a) Tsagogiorgas, C.; Wedel, J.; Hottenrott, M.; Schneider, M. O.; Binzen, U.; Greffrath, W.; Treede, R.-D.; Theisinger, B.; Theisinger, S.; Waldherr, R.; Krämer, B. K.; Thiel, M.; Schnuelle, P.; Yard, B. A.; Hoeger, S. N-octanoyl-dopamine is an agonist at the capsaicin receptor TRPV1 and mitigates ischemia-induced acute kidney injury in rat. *PLoS One* **2012**, *7*, e43525. (b) Waikar, S. S.; Liu, K. D.; Chertow, G. M. Diagnosis, epidemiology, and outcomes of acute kidney injury. *Clin. J. Am. Soc. Nephrol.* **2008**, *3*, 844−861.
(12) Westaway, S. M. The potential of transient receptor potential vanilloid type 1 channel modulators for the treatment of pain. *J. Med. Chem.* **2007**, *50*, 2589−2596.
(13) Klotz, S.; Pallavi, P.; Tsagogiorgas, C.; Zimmer, F.; Zollner, F. G.; Binzen, U.; Greffrath, W.; Treede, R. D.; Walter, J.; Harmsen, M. C.; Kramer, B. K.; Hafner, M.; Yard, B. A.; Hoeger, S. *N*-octanoyl dopamine treatment exerts renoprotective properties in acute kidney injury but not in renal allograft recipients. *Nephrol., Dial., Transplant.* **2016**, *31*, 564−573.
(14) Spindler, R. S.; Schnuelle, P.; Nickels, L.; Jarczyk, J.; Waldherr, R.; Theisinger, S.; Theisinger, B.; Klotz, S.; Tsagogiorgas, C.; Gottmann, U.; Kramer, B. K.; Yard, B. A.; Hoeger, S. N-octanoyl dopamine for donor treatment in a brain-death model of kidney and heart transplantation. *Transplantation* **2015**, *99*, 935−941.
(15) Milhazes, N.; Cunha-Oliveira, T.; Martins, P.; Garrido, J.; Oliveira, C.; Rego, A. C.; Borges, F. Synthesis and cytotoxic profile of 3,4-methylenedioxymethamphetamine ("Ecstasy") and its metabolites on undifferentiated PC12 cells: a putative structure-toxicity relationship. *Chem. Res. Toxicol.* **2006**, *19*, 1294−1304.
(16) Punna, S.; Meunier, S.; Finn, M. G. A hierarchy of aryloxide deprotection by boron tribromide. *Org. Lett.* **2004**, *6*, 2777−2779.
(17) (a) Stratford, M. R.; Riley, P. A.; Ramsden, C. A. Rapid halogen substitution and dibenzodioxin formation during tyrosinase-catalyzed oxidation of 4-halocatechols. *Chem. Res. Toxicol.* **2011**, *24*, 350−356. (b) Li, J.; Moe, B.; Vemula, S.; Wang, W.; Li, X. F. Emerging disinfection byproducts, halobenzoquinones: Effects of isomeric structure and halogen substitution on cytotoxicity, formation of reactive oxygen species, and genotoxicity. *Environ. Sci. Technol.* **2016**, *50*, 6744−6752.
(18) Darré, L.; Domene, C. Binding of capsaicin to the TRPV1 ion channel. *Mol. Pharmaceutics* **2015**, *12*, 4454−4465.
(19) Hottenrott, M. C.; Wedel, J.; Gaertner, S.; Stamellou, E.; Kraaij, T.; Mandel, L.; Loesel, R.; Sticht, C.; Hoeger, S.; Ait-Hsiko, L.; Schedel, A.; Hafner, M.; Yard, B.; Tsagogiorgas, C. N-octanoyl dopamine inhibits the expression of a subset of κB regulated genes: potential role of p65 Ser276 phosphorylation. *PLoS One* **2013**, *8*, e73122.
(20) Gillis, E. P.; Eastman, K. J.; Hill, M. D.; Donnelly, D. J.; Meanwell, N. A. Applications of fluorine in medicinal chemistry. *J. Med. Chem.* **2015**, *58*, 8315−8359.
(21) Wang, B.; Yang, F.; Shan, Y.-F.; Qiu, W.-W.; Tang, J. Highly efficient synthesis of capsaicin analogues by condensation of vanillylamine and acyl chlorides in a biphase $H_2O/CHCl_3$ system. *Tetrahedron* **2009**, *65*, 5409−5412.
(22) (a) Uchida, M.; Okazaki, K.; Mukaiyama, H.; Isawa, H.; Kobayashi, H.; Shiohara, H.; Muranaka, H.; Kai, Y.; Kikuchi, N.; Takeuchi, H.; Yokoyama, K.; Tsuji, E.; Ozawa, T.; Hoyano, Y.; Koizumi, T.; Misawa, K.; Hara, K.; Nakano, S.; Murakami, Y.; Okuno, H. Orally active factor Xa inhibitors: investigation of a novel series of 3-amidinophenylsulfonamide derivatives using an amidoxime prodrug strategy. *Bioorg. Med. Chem. Lett.* **2008**, *18*, 4682−4687. (b) Kolasa, T.; Miller, M. J. Synthesis of the chromophore of pseudobactin, a fluorescent siderophore from *Pseudomonas*. *J. Org. Chem.* **1990**, *55*, 4246−4255. (c) Lee, J. E.; Hitotsuyanagi, Y.; Kim, I. H.; Hasuda, T.; Takeya, K. A novel bicyclic hexapeptide, RA-XVIII, from *Rubia cordifolia*: structure, semi-synthesis, and cytotoxicity. *Bioorg. Med. Chem. Lett.* **2008**, *18*, 808−811. (d) Napolitano, A.; d'Ischia, M.; Costantini, C.; Prota, G. A new oxidation pathway of the neurotoxin 6-aminodopamine. Isolation and characterisation of a dimer with a tetrahydro[3,4a]iminoethanophenoxazine ring system. *Tetrahedron* **1992**, *48*, 8515−8522.
(23) Wilson, A. A.; Jin, L.; Garcia, A.; DaSilva, J. N.; Houle, S. An admonition when measuring the lipophilicity of radiotracers using counting techniques. *Appl. Radiat. Isot.* **2001**, *54*, 203−208.
(24) Test no. 117: Partition Coefficient (*n*-octanol/water), HPLC Method. *OECD iLibrary; OECD Guidelines for the Testing of Chemicals, Section 1. Physical-Chemical properties*; OECD: Paris, France, 2004. http://dx.doi.org/10.1787/9789264069824-en (accessed April 30, 2015).
(25) Zajac, D.; Spolnik, G.; Roszkowski, P.; Danikiewicz, W.; Czarnocki, Z.; Pokorski, M. Metabolism of *N*-acetylated-dopamine. *PLoS One* **2014**, *9*, e85259.
(26) Smit, N.; Tilgmann, C.; Karhunen, T.; Slingerland, R.; Ulmanen, I.; Westerhof, W.; Pavel, S. O-Methylation of L-dopa in melanin metabolism and the presence of catechol-O-methyltransferase in melanocytes. *Pigm. Cell Res.* **1994**, *7*, 403−408.
(27) Kiss, L. E.; Soares-da-Silva, P. Medicinal chemistry of catechol *O*-methyltransferase (COMT) inhibitors and their therapeutic utility. *J. Med. Chem.* **2014**, *57*, 8692−8717.
(28) (a) Tu, Z.; Li, S.; Sharp, T. L.; Herrero, P.; Dence, C. S.; Gropler, R. J.; Mach, R. H. Synthesis and evaluation of 15-(4-(2-[^{18}F]fluoroethoxy)phenyl)pentadecanoic acid: A potential PET tracer for studying myocardial fatty acid metabolism. *Bioconjugate Chem.* **2010**, *21*, 2313−2319. (b) Hendricks, J. A.; Keliher, E. J.; Marinelli, B.; Reiner, T.; Weissleder, R.; Mazitschek, R. In vivo PET imaging of histone deacetylases by ^{18}F-suberoylanilide hydroxamic acid (^{18}F-SAHA). *J. Med. Chem.* **2011**, *54*, 5576−5582.
(29) Morgan, P.; Maggs, J. L.; Page, P. C. B.; Park, B. K. Oxidative dehalogenation of 2-fluoro-17α-ethynyloestradiol in vivo. *Biochem. Pharmacol.* **1992**, *44*, 1717−1724.
(30) (a) Choi, J. Y.; Kim, C. H.; Jeon, T. J.; Kim, B. S.; Yi, C. H.; Woo, K. S.; Seo, Y. B.; Han, S. J.; Kim, K. M.; Yi, D. I.; Lee, M.; Kim, D. G.; Kim, J. Y.; Lee, K. C.; Choi, T. H.; An, G.; Ryu, Y. H. Effective microPET imaging of brain 5-HT(1A) receptors in rats with [^{18}F]MeFWAY by suppression of radioligand defluorination. *Synapse* **2012**, *66*, 1015−1023. (b) Rietjens, I. M. C. M.; Tyrakowska, B.; Veeger, C.; Vervoort, J. Reaction pathways for biodehalogenation of fluorinated anilines. *Eur. J. Biochem.* **1990**, *194*, 945−954.
(31) Grynkiewicz, G.; Poenie, M.; Tsien, R. Y. A new generation of Ca^{2+} indicators with greatly improved fluorescence properties. *J. Biol. Chem.* **1985**, *260*, 3440−3450.

DOI: 10.1021/acs.jmedchem.6b01191
J. Med. Chem. 2016, 59, 9855−9865